Available online at www.sciencedirect.com
ScienceDirect
Polymer 47 (2006) 6406–6413
polymer
www.elsevier.com/locate/polymer

Dielectric relaxation in montmorillonite/polymer nanocomposites

Kirt A. Page [a,*], Keiichiro Adachi [b]

[a] The University of Southern Mississippi, School of Polymers and High Performance Materials, 118 College Drive #10076, Hattiesburg, MS 39406, USA
[b] Department of Macromolecular Science, Graduate School of Science, Osaka University, Toyonaka, Osaka 560-0043, Japan

Received 23 February 2006; received in revised form 16 June 2006; accepted 19 June 2006
Available online 24 July 2006

Abstract

We report dielectric relaxation behavior in blends of sodium montmorillonite particles (MM) with a series of polymers (i.e., polyisoprene (PI), poly(propylene glycol) (PPG), and poly(butylene oxide) (PBO)). These polymers are known to exhibit the dielectric normal mode due to the fluctuation of the end-to-end vector as well as the segmental mode due to local, segmental fluctuations. The data indicate that all blend systems exhibit an additional relaxation process at a temperature region below the glass transition temperature, T_g, of the pure polymer component. The intensity of the new relaxation process increases with the content of MM and hence the relaxation process can be assigned to the segmental motion of the chains intercalated in the interlayers of MM. On the other hand, the relaxation time of the normal mode reflecting the fluctuation of the end-to-end vector is the same as the neat polymers but the intensity of the relaxation process increases due to enhancement of the internal electric field by MM.

Keywords: Dielectric relaxation; Nanocomposites; Type-A polymers

1. Introduction

Since the 1960s it has been known that various water-soluble polymers can intercalate into the interlayers, or van der Waals galleries, of crystalline aluminosilicates (i.e., clay) [1]. In the past decade, it was found that intercalation of hydrophobic polymers also occurs in mixtures of clays and molten polymers [2–5], and has been investigated extensively in industries for reinforcement of polymer/clay composites [6,7]. Among various clays, montmorillonite (MM) typically exhibits intercalation by organic compounds. For example, non-polar polymers such as polystyrene and polysiloxane can be accommodated between the interlayers of MM. Chain dynamics of polymers confined in the gallery spaces of clays has been studied by various methods including nuclear magnetic resonance (NMR) [8,9], dielectric relaxation spectroscopy (DRS) [10], rheology [11,12], gas permeation [13], and computer simulation [14]. Anastasiadis et al. [10] reported the dielectric relaxation in clay/polysiloxane systems and found that the polymer chains located in the galleries move faster than the bulk, pure polymer. The results were explained in terms of the effects of confinement of the chains in narrow spaces [15–17]. The structure of the suspensions of organically modified MM in toluene and acetone was investigated by Vaia et al. [18]. They found that when the content of the MM is low (5 wt%), the MM crystal is dispersed in a form of the monolayer or stacks of several layers.

The aim of this paper is to study the effect of intercalation on the local and global motions of polymer chains in polymer/MM systems with relatively low content of MM. To date many studies have focused on polymer/MM nanocomposites that have used montmorillonite in which the sodium ions on the surface of the gallery spaces are replaced by organo-ammonium counterions. This type of modification allows for ease of intercalation by hydrophobic organic molecules such as polymers. However, it has also been reported that polymers (i.e., poly(ethylene oxide)) can also intercalate unmodified sodium MM [19–21]. Lin et al. [19] have reported that

* Corresponding author. Present address: National Institute of Standards and Technology, Polymers Division, Building 224/Room B220, 100 Bureau Drive MS8542, Gaithersburg, MD 20899-8540, USA. Tel.: +1 301 975 5030; fax: +1 301 975 4924.
E-mail address: kirt.page@nist.gov (K.A. Page).

0032-3861/$ - see front matter © 2006 Elsevier Ltd. All rights reserved.
doi:10.1016/j.polymer.2006.06.042

poly(propylene oxide) bearing amine groups at the chain ends can intercalate the gallery spacing of unmodified sodium MM. Yoshimoto et al. [21] have also reported the intercalation of unmodified sodium MM by polymer chains. Moreover, it has also been shown that unmodified sodium MM can be easily intercalated by low molecular weight organic compounds to form nanocomposites [22]. We have chosen *cis*-polyisoprene (PI), poly(propylene glycol) (PPG), and poly(butylene oxide) (PBO) as the polymer components in our composite systems. Although it is unlikely that these polymers can lead to completely exfoliated nanocomposites, it is likely that they form significantly intercalated systems as demonstrated in the literature. All of these polymers posses type-A dipoles aligned parallel to the chain contour as well as type-B dipoles aligned perpendicular to the chain contour [23,24]. As is well known, polymers having type-A dipoles exhibit the dielectric normal mode relaxation, which reflects the fluctuation of the end-to-end vector, but those having type-B dipoles exhibit the dielectric segmental mode relaxation, which reflects local motions [23]. The dielectric relaxation behavior of bulk PI [23,25–27], PPG [28–30], and PBO [31] has been reported by several scientists. The objective of the present study is to examine how the normal and segmental modes of these polymer chains are affected by the presence of MM particles.

2. Experimental section

2.1. Materials

Pure sodium montmorillonite (MM) (commercial name: Kunipia-F) was supplied by Kunimine Industries Co. (Tokyo, Japan), and has the structure $Na_{2/3}Si_8(Al_{10/3}Mg_{2/3})O_{20}(OH)_4$. *cis*-Polyisoprene (PI) was synthesized by anionic polymerization in heptane with *sec*-butyllithium. The average molecular weight (M_w) and the polydispersity (M_w/M_n) were determined by gel permeation chromatography (Tosoh LS-8000, Tokyo, Japan) equipped with a light scattering detector and were found to be 14,900 and 1.08, respectively. Poly(propylene glycol) (PPG) with $M_w = 2900$ and $M_w/M_n = 1.1$ was obtained from Wako Chemicals Inc. (Tokyo, Japan). According to Hayakawa and Adachi [28], the PPG has a bifurcated structure (i.e., the direction of the type-A dipoles is inverted at the center of the molecules). Poly(butylene oxide) (PBO) was synthesized by polymerization of butylene oxide in tetrahydrofuran (THF) with potassium hydride [31]. The PBO was fractionated by using THF and methanol, and the fraction with $M_w = 4500$ and $M_w/M_n = 1.21$ was employed. PI and MM were mixed in hexane solutions and the hexane was removed under vacuum. Due to the low viscosity of the PPG and PBO, the MM/PPG and MM/PBO blends were prepared by direct mixing.

2.2. Dielectric relaxation spectroscopy

Dielectric measurements were carried out on an RLC Digibridge (Quadtech 1693, Maynard, USA) in the frequency range of 10 Hz and 2 MHz and over a temperature range from 80 to 400 K. A guarded capacitance cell was used for the measurements on viscous liquids and has been previously reported [27].

3. Results and discussion

3.1. MM/PI system

Fig. 1(A–B) shows the temperature dependence of ε' and ε'' at 0.1, 1, and 10 kHz, respectively. Three loss maxima can be seen in Fig. 1B and the corresponding dispersions of ε' are shown in Fig. 1A. These relaxation processes are termed as α_n, α_s, and α_s' from the high temperature side. The ε'' curves of MM/PI(10/90) and PI are compared at 1 kHz in Fig. 2. The high and low temperature ε'' peaks of pure PI are assigned to the normal mode (α_n) and segmental mode (α_s), respectively [23]. Since these peak temperatures agree with the loss peak temperatures for pure PI, α_n and α_s processes are assigned to the normal mode and segmental mode, respectively. However, the intensities of α_n and α_s processes are much higher than those of the pure PI, which will be addressed later.

The α_s' process observed in the composite occurs at approximately 190 K, which is below the glass transition temperature, T_g, of pure PI (200 K), and is not seen in pure PI.

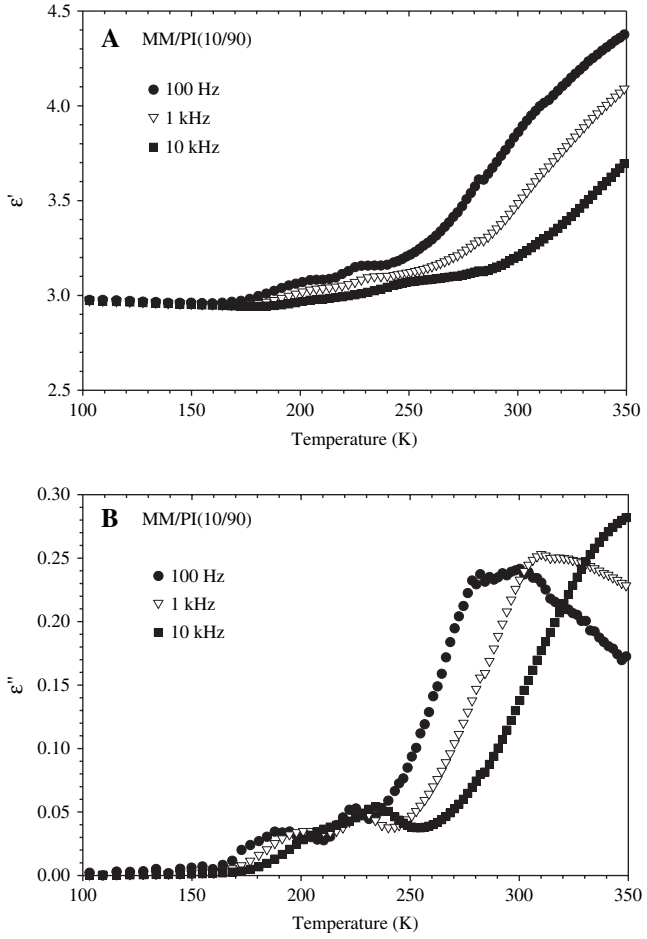

Fig. 1. Temperature dependence of ε' (A) and ε'' (B) for MM/PI(10/90).

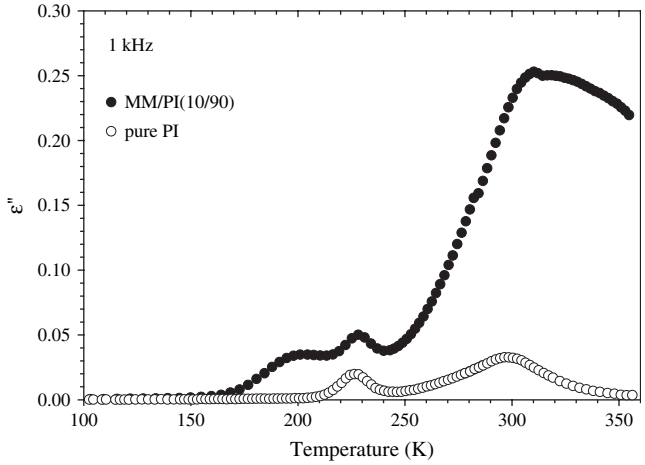

Fig. 2. Temperature dependence of ε'' for MM/PI(10/90) compared to pure PI.

In order to assign the mechanism of this relaxation process, the relaxation behavior of MM/PI with different MM content, namely MM/PI(5/95), was examined. By examining Cole–Cole plots, it was found that the relaxation strength $\Delta\varepsilon$ for the α_s' process is proportional to the content of MM, which indicates that the α_s' process is due to motions of the PI adsorbed to the MM. The shorter relaxation time for the α_s' process compared to the segmental mode of pure PI can be explained in terms of the effect of confinement as reported by Anastasiadis et al. [10]. The α_s' will be discussed in further detail later.

Fig. 3(A–C) shows the frequency dependence of ε'' for the α_s', α_s, and α_n processes, respectively. From the Cole–Cole plots, the relaxation strengths $\Delta\varepsilon$ were determined. The $\Delta\varepsilon$'s for the α_s', α_s, and α_n processes of the MM/PI(10/90) sample were 0.22, 0.33, and 1.6, respectively, and those of the MM/PI(5/95) sample were 0.085, 0.24, 0.70, respectively. The error in the determination of $\Delta\varepsilon$ was approximately ±30%. From these data, it is apparent that the relaxation strengths for the α_s' and α_n processes are approximately proportional to the content of the clay.

Fig. 4 shows Arrhenius plots for the loss maximum frequencies, f_m, for the α_s', α_s, and α_n processes of MM/PI(10/90) and MM/PI(5/95). The α_s and α_n processes are shown to exhibit the Vogel–Fulcher type behavior [32,33], indicating a cooperative relaxation behavior; however, the Arrhenius plot for the α_s' process is linear and results in an activation energy of 50.1 kJ mol^{-1}. The plots for the systems containing 5% and 10% clay coincide well, indicating that the relaxation times for all processes are independent of the content of MM.

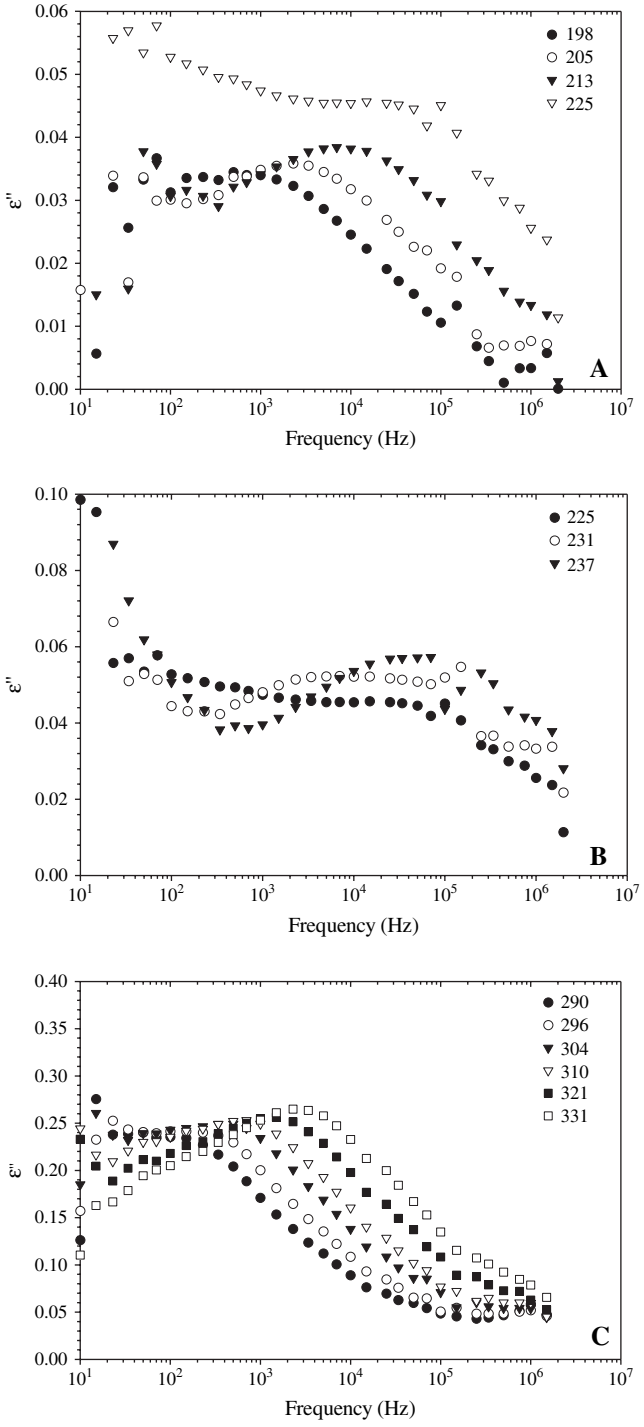

Fig. 3. Frequency dependence of ε'' for MM/PI(10/90) in the (A) α_s' relaxation region, (B) α_s relaxation region, and (C) α_n relaxation region.

3.2. MM/PPG system

Fig. 5(A–D) shows the temperature dependence of ε' and ε'' for MM/PPG(10/90) and MM/PPG(20/80). Three loss (ε'') peaks are observed as in the case for the MM/PI system. Fig. 6 compares the temperature dependence of ε'' for MM/PPG(10/90) with that of pure PPG. The two peaks seen in pure PPG have been assigned to the normal mode, α_n, and the local segmental mode, α_s, in the order of decreasing temperature [28]. In the ε'' curve of MM/PPG(10/90), the loss peaks at the highest temperature and that of the middle temperature occur at the same temperatures as those for pure PPG and therefore can be assigned to the α_n and α_s processes, respectively. The ε'' peak at the lowest temperature, termed α_s', is not seen in the pure PPG and occurs below the T_g of PPG (200 K). Comparing the ε'' curves of MM/PPG(10/90) and MM/PPG(20/80), we see that the temperatures of the loss maxima are independent of the MM content. The intensity

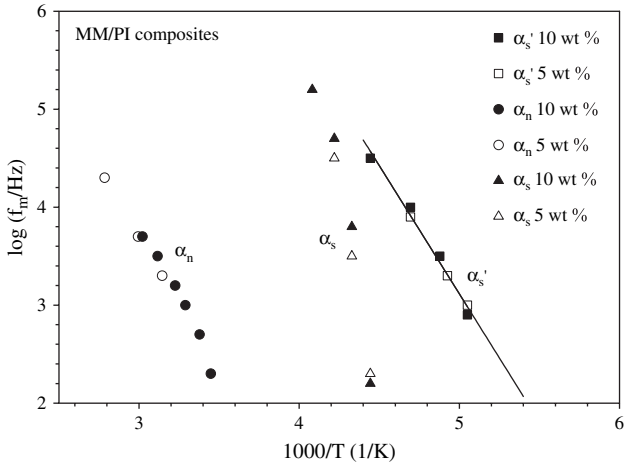

Fig. 4. Arrhenius plots for the α_n, α_s, and α_s' processes for MM/PI composites of 10 and 5 wt.% clay content.

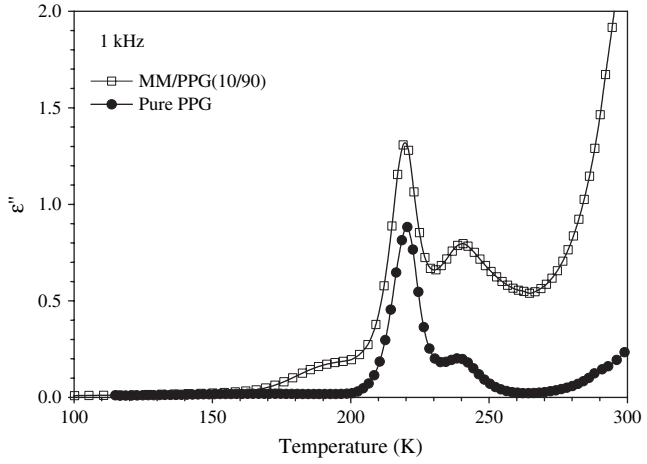

Fig. 6. Temperature dependence of ε'' for MM/PPG(10/90) compared to pure PPG.

of the α_s' process for MM/PPG(20/80) is about two times higher than that of MM/PPG(10/90), indicating that the α_s' process is due to the relaxation process associated with motions of PPG chains confined in the gallery spaces of the MM. On the other hand the intensities of α_n and α_s do not change much with an increase in the MM content. However, in Fig. 6 it can be seen that the ε'' of the MM/PPG(10/90) blend is much higher than that of pure PPG, which is similar to that observed for the MM/PI system.

The frequency dependence of ε'' in the α_s' relaxation region of MM/PPG(20/80) blend is shown in Fig. 7, which shows a single relaxation peak. As the temperature is increased, there is a shift in the peak maximum to higher frequencies. Fig. 8 shows the corresponding Arrhenius plot for the α_s' process,

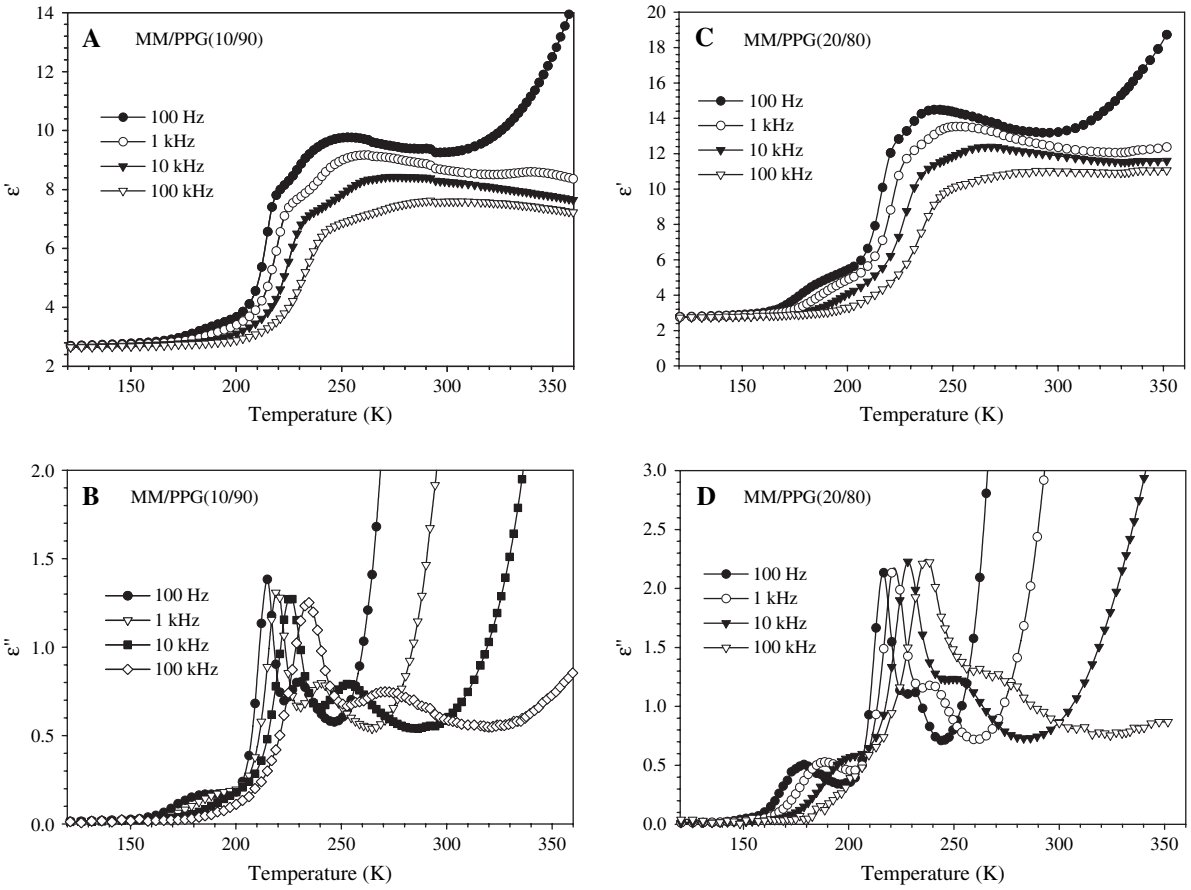

Fig. 5. Dielectric constant, ε', and loss, ε'', for the MM/PPG composite systems: (A) ε' of MM/PPG(10/90), (B) ε'' of MM/PPG(10/90), (C) ε' of MM/PPG(20/80) and (D) ε'' of MM/PPG(20/80).

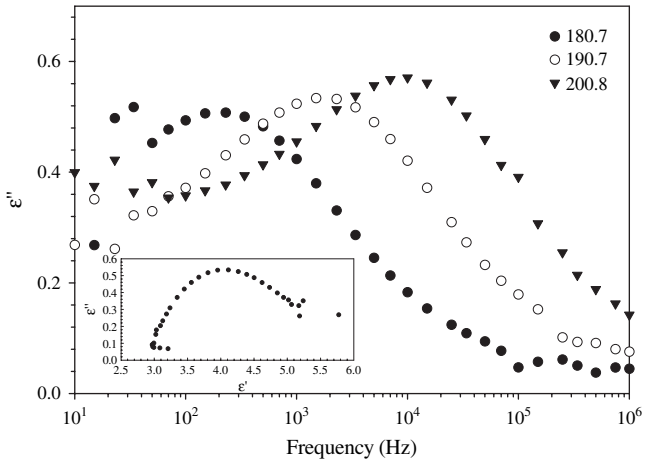

Fig. 7. Frequency dependence of ε'' for MM/PPG(20/80) in the α_s' relrelaxation region. Inset indicates the Cole–Cole plot at 190.7 K.

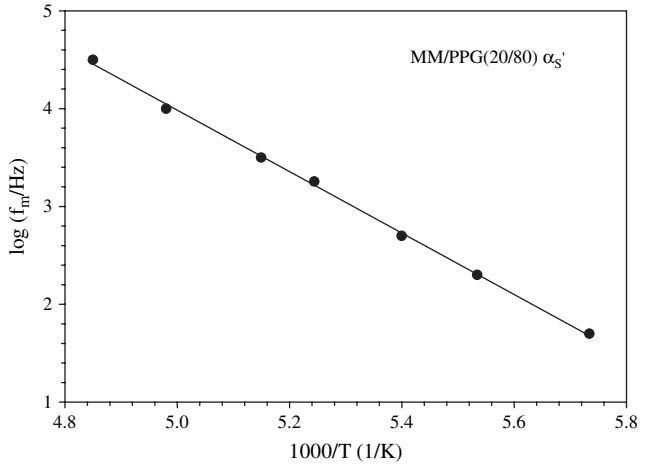

Fig. 8. Arrhenius plot for the α_s' process for the MM/PPG(20/80) composite.

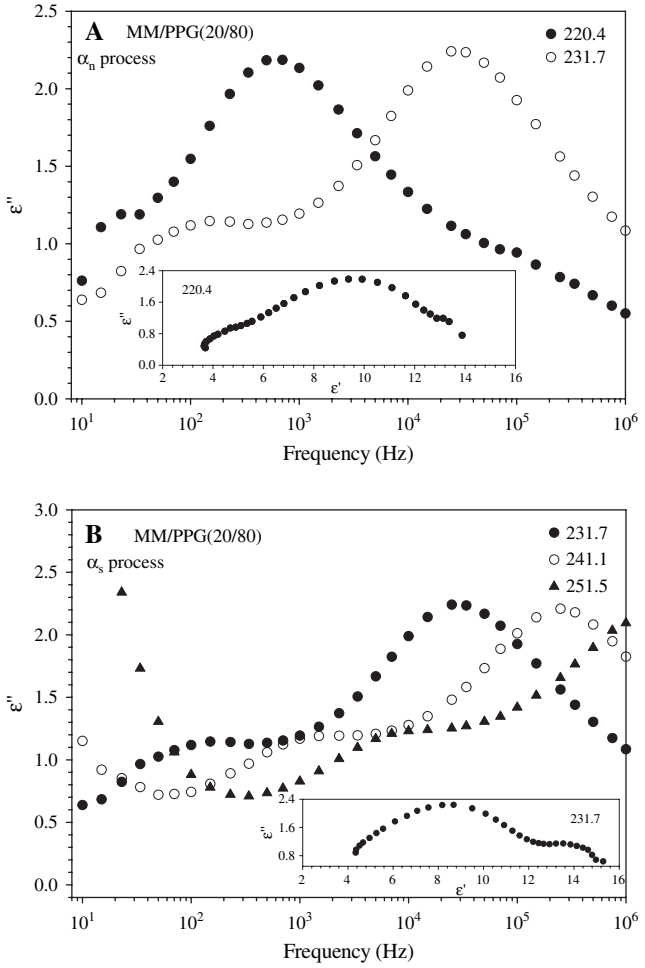

Fig. 9. Frequency dependence of ε'' for MM/PPG(20/80) in the region of the (A) α_s and (B) α_n relaxation processes. Inset indicates the Cole–Cole plots at (A) 220.4 K and (B) 231.7 K.

which conforms to a straight line, and has an activation energy of 56 kJ mol^{-1}. As observed for the MM/PI system, the mechanism of molecular motions for the α_s' process is different from the segmental mode of bulk polymers which conforms to the Vogel–Fulcher equation [32,33].

Fig. 9(A–B) shows the frequency dependence of ε'' in the region of the (a) α_n and (b) α_s processes. The shape of the loss curves is similar to those of pure PPG but the intensities are several times higher than pure PPG. From Cole–Cole plots, seen as insets in Figs. 7 and 9, the relaxation strengths for all three processes were determined to be 2.8 ± 0.3 (α_s'), 12.0 ± 3 (α_s), and 3.0 ± 1 (α_n).

3.3. MM/PBO system

Fig. 10 shows the temperature dependence of ε' and ε'' for MM/PBO(10/90). As observed for MM/PI and MM/PPG systems, three loss peaks can be seen in the plots of ε'' versus temperature. Fig. 11 compares the ε'' curves of MM/PBO(10/90) and pure PBO. The peak at the highest temperature and the middle temperature can be assigned to the normal mode (α_n) and segmental mode (α_s), respectively [31]. Again, this behavior is very similar to that observed for the MM/PI and MM/PPG blend systems and the loss peaks are labeled as α_n, α_s, and α_s' from the high temperature side. The small shoulder seen on the low temperature side of the segmental mode is the α_s' process and occurs below the T_g of pure PBO (193 K). This behavior is very similar to the MM/PI and MM/PPG systems. As also observed for the MM/PI and MM/PPG systems, the intensities of α_n and α_s processes are higher than those of pure PBO. For the sake of comparison, the ε'' curves for MM/PI(10/90) and MM/PPG(10/90) are also plotted in Fig. 11. It is can be seen that the α_s' relaxations of the three systems are located in the same temperature region. The peak temperatures of the α_s' relaxation at 1 kHz are 198 ± 1, 190 ± 3, and 188 ± 3 K for the MM/PI, MM/PPG, and MM/PBO systems, respectively. These temperatures are approximately 30 K below the α_s relaxation temperatures of the pure polymer samples. This indicates that the segmental motions are accelerated by intercalation as pointed out above. It is also seen that the intensities of the ε'' of the three systems are quite different, reflecting the dipole moments of PI, PPG, and PBO. This ensures that the α_s' relaxation is not due to the

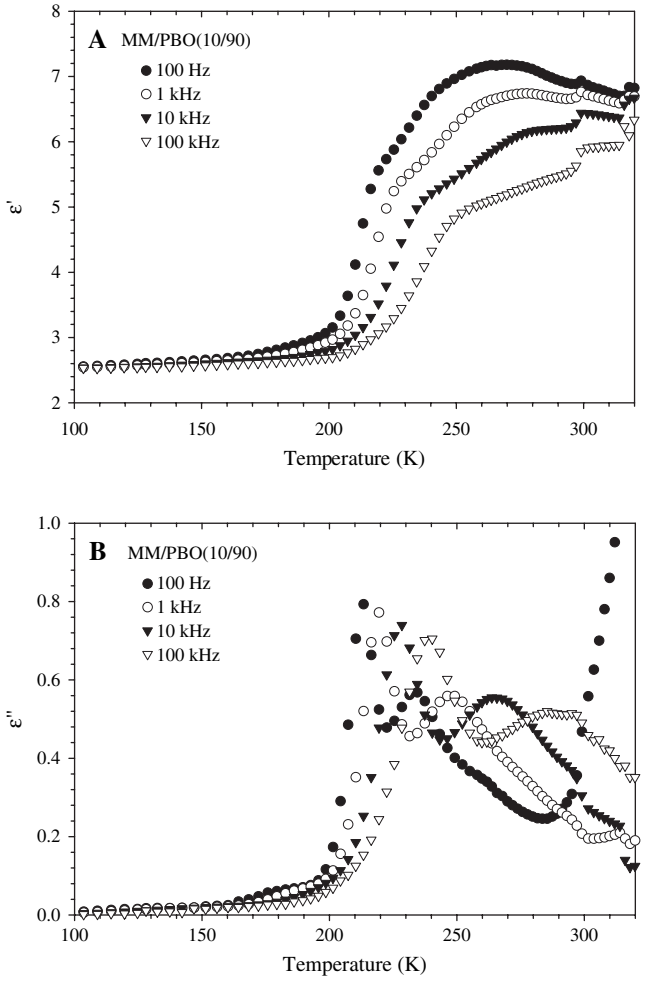

Fig. 10. Temperature dependence of ε' (A) and ε'' (B) for MM/PBO(10/90).

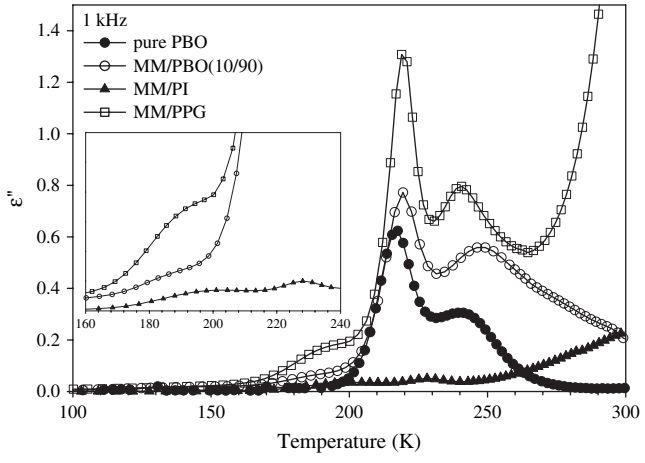

Fig. 11. Temperature dependence of ε'' for MM/PBO(10/90) compared to pure PBO. For the sake of comparison, the ε'' curves of MM/PI(10/90) and MM/PPG(10/90) are also plotted. The plots of the α_s and α_s' relaxation are magnified in the inset.

MM particles since the contents of the MM compared here are the same.

Fig. 12(A–B) shows the frequency dependence of ε'' in (a) the region of the α_s' process and (b) in the region of the

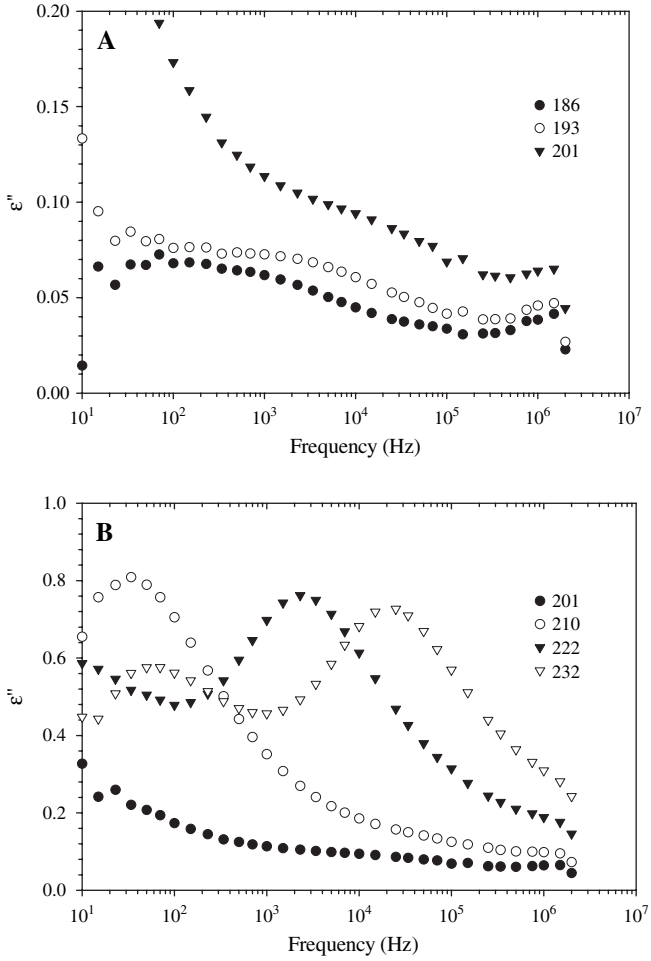

Fig. 12. Frequency dependence of ε'' for MM/PBO(10/90) in (A) the region of the α_s' process and (B) the region covering the α_s to α_n relaxation processes.

overlapping of α_s to α_n region. In Fig. 12A, we see that the α_s' process exhibits a broad relaxation spectrum. Comparing the broadness of the α_s' loss peaks among the three MM/polymer systems, we conclude that the distribution of relaxation times for the segmental motions of polymers confined in narrow van der Waals galleries depends strongly on the structure and size of the monomeric units.

3.4. Relaxation mechanism of intercalated chains

In the above sections it has been found that all three blend systems examined exhibit the α_s' process just below the T_g of the corresponding bulk polymers. This suggests that the α_s' process generally occurs irrespective of the chemical structure and intermolecular interactions of the polymers. Anastasiadis et al. [10] reported the dielectric relaxation in clay/polymethylphenylsiloxane systems with the polymer concentration ranging from 15 to 30 wt%, where the clays were hectorite and montmorillonite modified with dimethyldioctadecyl ammonium. Due to the low content of the polymer, it was assumed that a majority of the polymer chains were intercalated. It was reported that the segmental relaxation time of the polysiloxane confined in the clay galleries was much

shorter than for the bulk, pure polymer and also that the temperature dependence was weaker [10]. The shortened relaxation times of the confined chains were compared to that of simple molecules confined in pores of materials such as zeolites [15–17] and explained as a decrease in the cooperative nature of the segmental motions. The α_s' processes observed in the present study show very similar results.

In the present study, sodium MM (not modified by organic compounds) was used. The similarity in the dielectric relaxation behavior of the materials in this study and those studied by Anastasiadis et al. [10] indicates that the organo-modification of the MM is not the origin of the faster relaxation time of the α_s' processes. In light of these results it is necessary to clarify how segmental motions occur in a confined geometry. Several authors have proposed models to describe the local motions of polymer chains [34–41], including the crankshaft [34,35,40,41], or three-bond motions [38,39]. The crankshaft-like motion is accompanied by the internal rotation around two bonds; hence the activation energy is twice that of the barrier height for internal rotation. It is expected that in a narrow gallery, relatively small crankshaft-like motions, or three-bond motions, are the dominant mechanism of local conformation changes. The PPG chains contain both C–C and C–O bonds, with barrier heights for internal rotation determined by molecular dynamics [42] to be 22 and 46 kJ mol^{-1} (an average of 32 kJ mol^{-1}), respectively. The activation energy for the smallest crankshaft of $(T-G)_3$ conformation—where T and G indicate the *trans* and *gauche* conformations, respectively—can be formed with either two C–C bonds or two C–O bonds. Therefore the activation energy is expected to be intermediate of 44 and 92 kJ mol^{-1}. The activation energy for a three-bond jump cannot be calculated easily, but as pointed out by Boyer [43] it is similar to that for the crankshaft-like motion. As described above, the activation energy for the α_s' process of the MM/PPG(20/80) blend is 56 kJ mol^{-1}, which is slightly less than twice the average of the barrier height for the two bonds. In PI the four carbon atoms C1–C2=C3–C4 are on the same plane and form a virtual bond; hence the conformational changes occur through the internal rotation around the C–C bond connecting the C4 and C1 of a neighboring monomer unit and has a barrier height of ca. 26.8 kJ mol^{-1}. The observed activation energy for the α_s' for the MM/PI(10/90) system is ca. 51 kJ mol^{-1}, which is approximately twice the barrier height for this rotation, thus lending credit to the assigned mechanism proposed in this study and by Anastasiadis et al. [10].

One of our interests was to clarify the behavior of the normal mode relaxation of intercalated polymer chains. In the two dimensional spaces, the chain segments cannot cross each other and therefore it is expected that the dynamics slows down. It is expected that the normal mode relaxation of intercalated chains obeys the repetition mechanism [44] rather than the Rouse model [45]; however, the present polymer samples have a molecular weight lower than the characteristic molecular weight [46]. However, such a behavior has not been detected here. It is likely that the normal mode of the intercalated chains occurs at a high temperature and low frequency, where the dielectric loss due to DC conduction overwhelms the signal of the dipolar relaxation.

3.5. The α_n and α_s processes

The dielectric loss peaks for the α_n and α_s processes in all MM/polymer systems were observed at the same temperatures/frequencies as those for the pure polymers. Therefore, the α_n and α_s processes can be assigned to the normal and segmental mode relaxations of the chains located outside the MM particles. The higher intensities of ε'' for the composites compared to the pure polymers are puzzling. We speculate that the enhancement of the intensity is due to enhancement of the internal field. However, at the present stage no information is available on the electric properties of MM. This problem is an issue to be studied in the future.

4. Conclusions

We have studied the dielectric behavior for composites of sodium montmorillonite (MM) with a series of polymers (i.e., polyisoprene (PI), poly(propylene glycol) (PPG), and poly(butylene oxide) (PBO)). For all the systems, three relaxation processes are observed and termed α_n, α_s, and α_s' from the high temperature side. The temperature dependence curves of the dielectric loss factor, ε'', indicate that the ε'' peaks for the α_n and α_s processes are located at temperatures where the normal mode and the local segmental mode are observed for the corresponding pure polymers. Thus the α_n and α_s processes have been assigned to motions of polymer chains located outside the MM particles. However, the relaxation strengths for the α_n and α_s processes are much higher than those for the pure polymers due to enhancement of the internal field by the presence of the MM. The α_s' process is observed only in the composites and occurs below the T_g of the corresponding pure polymer. Since the relaxation strength for the α_s' process has been shown to be approximately proportional to the content of MM, this process has been attributed to segmental motions of the intercalated polymer chains. The faster mobility for the α_s' process can be explained in terms of the effect or confinement in the narrow galleries of the MM. The Arrhenius plot for the α_s' process is linear and the activation energies for the α_s' process of MM/PI(10/90) and MM/PPG(20/80) are 51 and 56 kJ mol^{-1}, respectively, which are about twice the barrier height for internal rotation around the skeletal bonds. This indicates segmental motions without the effect of entanglement. The normal mode of the intercalated chains is not observed since it occurs at high temperature and low frequency, where the dielectric loss due to DC conduction overwhelms the signal of the dipolar relaxation.

Acknowledgments

This material is based upon work supported by the National Science Foundation (NSF) under grant no. 0412307. Any opinions, findings, and conclusions or recommendations expressed in this material are those of the author(s) and do

not necessarily reflect the views of the National Science Foundation. The authors gratefully acknowledge the contributions of the Japan Society for the Promotion of Science to the NSF East Asia Graduate Fellowship program. Kirt Page would like to thank his Ph.D. advisor, Dr. Robert Moore, at The University of Southern Mississippi for allowing him to take the summer to study in Japan under Dr. Adachi's guidance.

References

[1] Theng BKG. Formation and properties of clay–polymer complexes. In: Developments in soil science, vol. 9. New York: Elsevier Scientific; 1979.
[2] Giannelis EP. Adv Mater 1996;8(1):29.
[3] Ren JX, Krishnamoorti R. Macromolecules 2003;36(12):4443–51.
[4] Vaia RA, Jandt KD, Kramer EJ, Giannelis EP. Macromolecules 1995; 28(24):8080–5.
[5] Vaia RA, Sauer BB, Tse OK, Giannelis EP. J Polym Sci Part B Polym Phys 1997;35(1):59–67.
[6] Kim Y, White JL. J Appl Polym Sci 2004;92(2):1061–71.
[7] Kwiatkowski J, Whittaker AK. J Polym Sci Part B Polym Phys 2001; 39(14):1678–85.
[8] Harris DJ, Bonagamba TJ, Schmidt-Rohr K. Macromolecules 1999; 32(20):6718–24.
[9] Sahoo SK, Kim DW, Kumar J, Blumstein A, Cholli AL. Macromolecules 2003;36(8):2777–84.
[10] Anastasiadis SH, Karatasos K, Vlachos G, Manias E, Giannelis EP. Phys Rev Lett 2000;84(5):915–8.
[11] Gu SY, Ren J, Wang QF. J Appl Polym Sci 2004;91(4):2427–34.
[12] Ray SS, Okamoto M. Prog Polym Sci 2003;28(11):1539–641.
[13] Grunlan JC, Grigorian A, Hamilton CB, Mehrabi AR. J Appl Polym Sci 2004;93(3):1102–9.
[14] Kuppa V, Foley TMD, Manias E. Eur Phys J 2003;12(1):159–65.
[15] Huwe A, Kremer F, Behrens P, Schweiger W. Phys Rev Lett 1999; 82(11):2338–41.
[16] Pissis P, Kyritsis A, Daoukaki D, Barut G, Perster R, Nimtz G. J Phys Condens Matt 1998;10(28):6205–27.
[17] Schonhals A, Stauga R. J Chem Phys 1998;108(12):5130–6.
[18] Vaia RA, Liu W, Koerner H. J Polym Sci Part B Polym Phys 2003; 41(24):3214–36.
[19] Lin J-J, Cheng I-J, Wang R, Lee R-J. Macromolecules 2001;34(26): 8832–4.
[20] Paul M-A, Alexandre M, Degee P, Henrist C, Rulmont A, Dubois P. Polymer 2003;44:443–50.
[21] Yoshimoto S, Ohashi F, Kameyama T. Solid State Commun 2005;136: 251–6.
[22] Lepoittevin B, Pantoustier N, Devvalckenaere M, Alexandre M, Kubies D, Calberg C, et al. Macromolecules 2002;35(22):8385–90.
[23] Adachi K, Kotaka T. Prog Polym Sci 1993;18(3):585–622.
[24] Stockmayer WH. Pure Appl Chem 1967;15:539–54.
[25] Adachi K, Kotaka T. Macromolecules 1985;18(3):466–72.
[26] Boese D, Kremer F. Macromolecules 1990;23(3):829–35.
[27] Imanishi Y, Adachi K, Kotaka T. J Chem Phys 1988;89(12):7585–92.
[28] Hayakawa T, Adachi K. Polymer 2001;42(4):1725–32.
[29] Schonhals A. Macromolecules 1993;26(6):1309–12.
[30] Stockmayer WH, Baur ME. J Am Chem Soc 1964;86(17):3485–9.
[31] Kyritsis A, Pissis P, Mai SM, Booth C. Macromolecules 2000;33(12): 4581–95.
[32] Fulcher GS. J Am Ceram Soc 1925;8:339.
[33] Vogel H. Phys. Z. 1921;22:645.
[34] Hall CK, Helfand E. J Chem Phys 1982;77(6):3275–82.
[35] Helfand E. J Chem Phys 1971;54(11):4651–61.
[36] Jones AA, Stockmayer WH. J Polym Sci Part B Polym Phys 1977;15(5): 847–61.
[37] Monnerie L, Geny F. J Chim Phys 1969;66:1691–7.
[38] Valeur B, Jarry JP, Geny F. J Polym Sci Part B Polym Phys 1975;13(4): 667–74.
[39] Valeur B, Monnerie L, Jarry JP. J Polym Sci Part B Polym Phys 1975; 13(4):675–82.
[40] Schatzki TF. J Polym Sci 1962;57:496.
[41] Schatzki TF. Polymer 1965;6:646. Preprints.
[42] Burkert U, Allinger NL. Molecular mechanics. Washington, D.C.: American Chemical Society; 1982. p. 340.
[43] Boyer RF. Rubber Chem Technol 1963;34:1303.
[44] De Gennes PG. J Chem Phys 1971;55(2):572–9.
[45] Rouse PE. J Chem Phys 1953;21(7):1271–80.
[46] Ferry JD. Viscoelastic properties of polymers. 3 ed. New York: John Wiley & Sons; 1980. p. 641.